

Radiative corrections for muon physics

Robert Szafron



Precision Radiative Corrections
for Next Generation Experiments Workshop
May 16-19, 2016
Jefferson Lab

Motivation

- Muon physics is a great place for developing tools and methods that can be used elsewhere
- Muons serve well as a QED laboratory
- Clean theoretical framework — perturbative and well measured
- Easy to test complicated QCD objects/EFT

Results and methods

- ★ 2 loops muon decay spin asymmetry
(F. Caola, A. Czarnecki, Y. Liang, K. Melnikov, R.S.)
- ★ Bound muon decay spectrum in the shape function region (A. Czarnecki, M. Dowling, X. Garcia i Tormo, W. J. Marciano, R.S.)
- ★ Bound muon decay spectrum close to the endpoint (R.S., A. Czarnecki)
- ◆ Structure function
- ◆ Perturbative fragmentation function
- ◆ Shape function
- ◆ HQEFT
- ◆ Sector decomposition
- ◆ Jet algorithm
- ◆ Region expansion

Part I

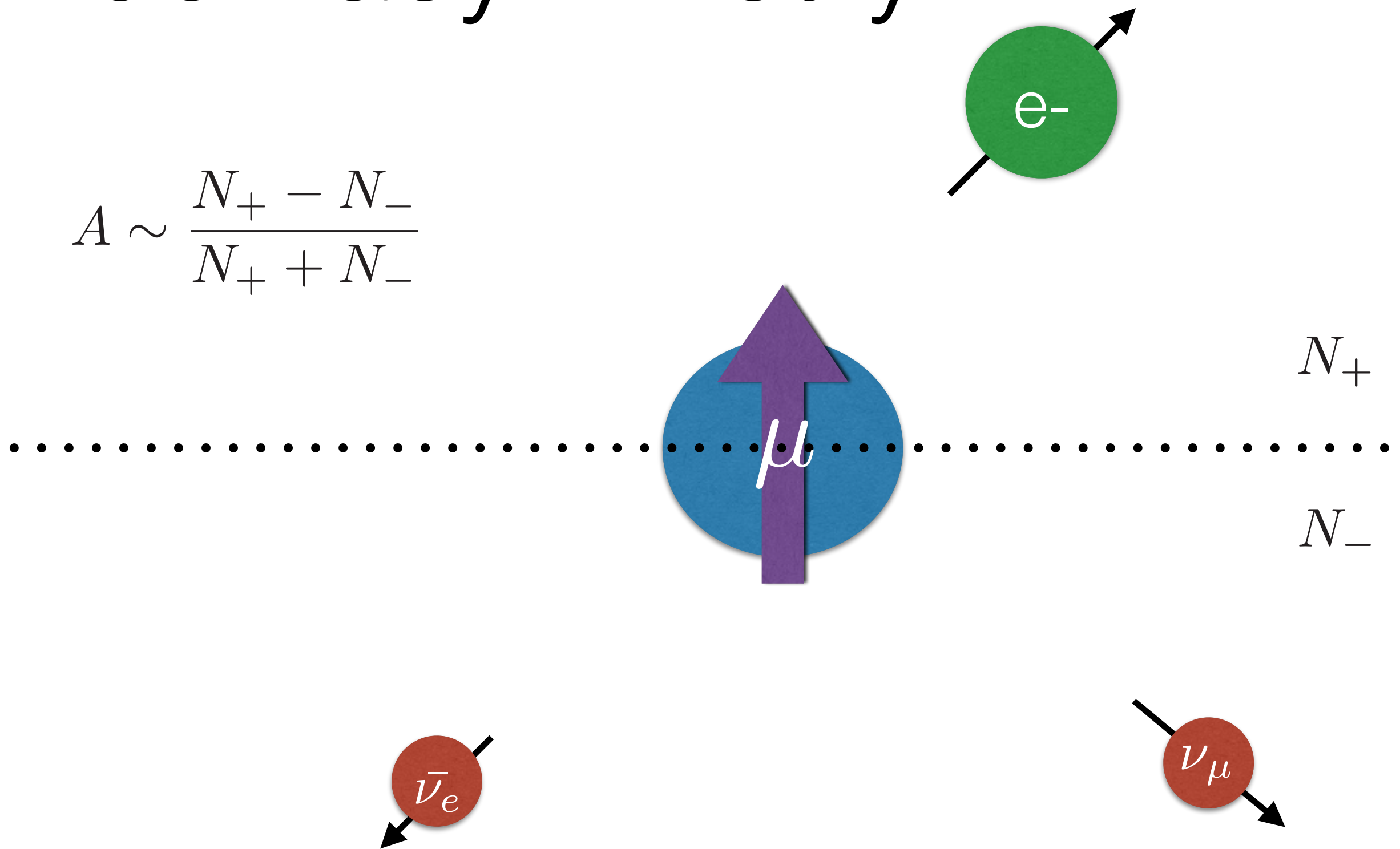
Muon spin asymmetry

or

What we can learn from
QCD about asymmetry?

Muon asymmetry

$$A \sim \frac{N_+ - N_-}{N_+ + N_-}$$



Muon decay asymmetry

- Measured in TWIST experiment in TRIUMF (2011)
- NLO with electron mass dependence calculated in 2001 by Arbuzov
 - Note that the NNLO correction to the total decay width was known since 1999 (van Ritbergen, Stuart)
- Useful to study V-A structure of interaction

NNLO asymmetry

- We used method developed in pQCD to extract soft and collinear divergences in a systematic way.
 - sector decomposition
 - phase-space partitioning
- There is an intrinsic ambiguity in the spin asymmetry at the NNLO
- The ambiguity is related to the e^+e^- pair production

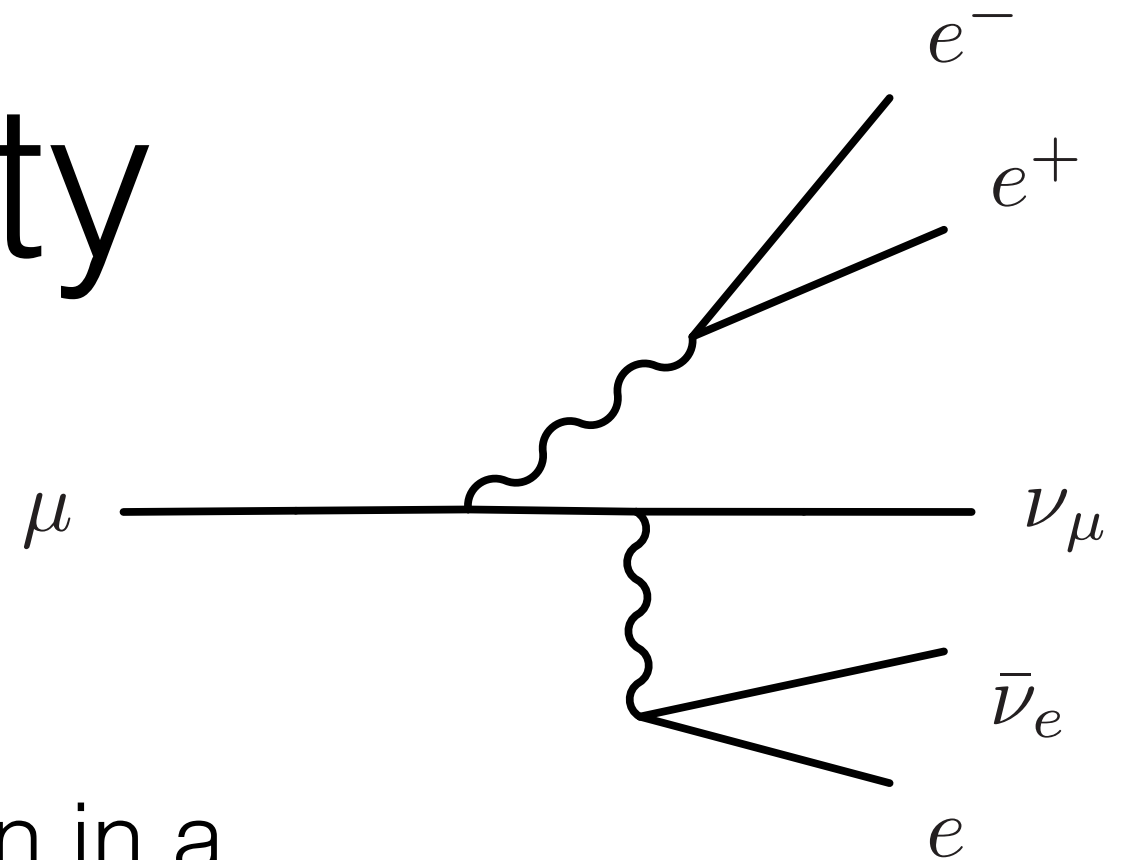
Czakon, 2010

Some technical remarks

- Amplitudes were calculated using spinor helicity formalism
- Subtraction terms are lower order amplitudes with appropriate splitting function (or eikonal factors)
- Framework developed for fully differential decays of heavy quarks was used

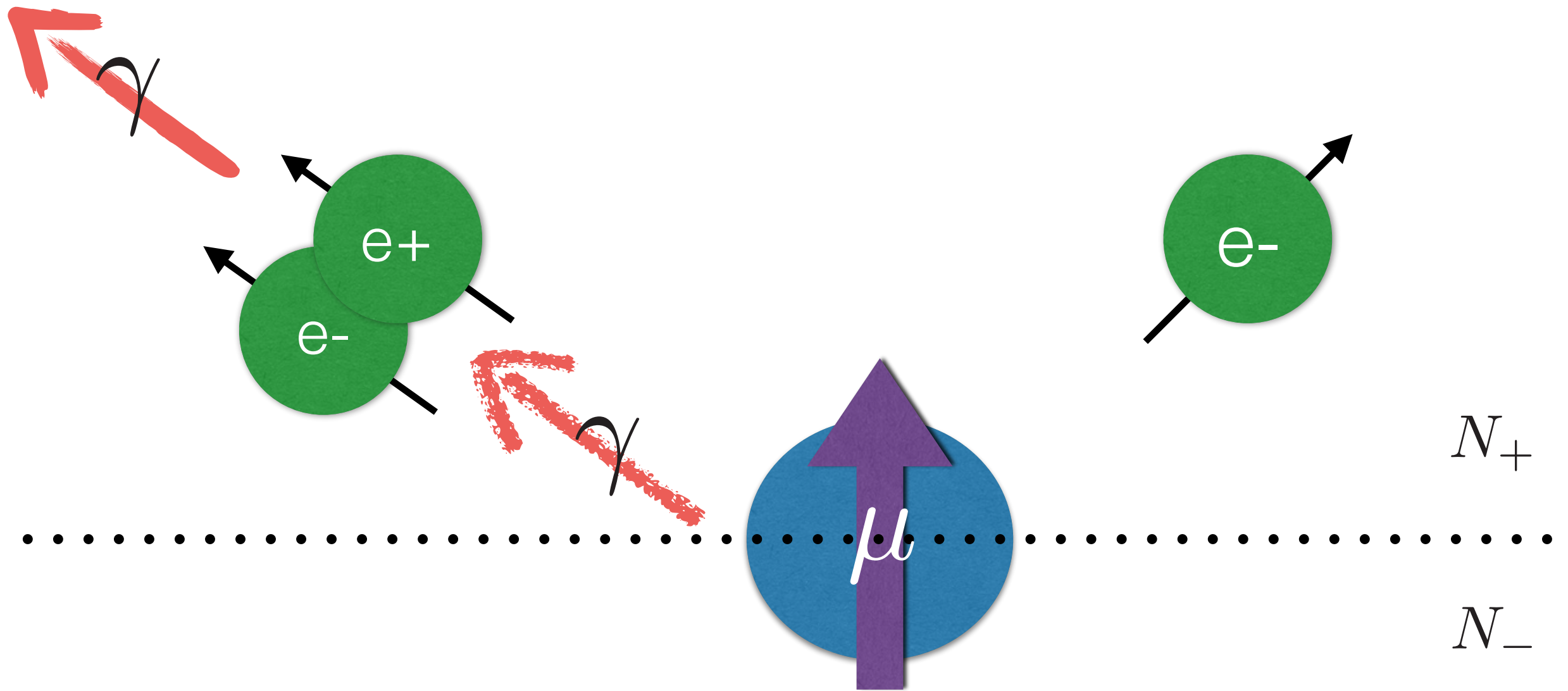
Brucherseifer, Caola, Melnikov, 2013

NNLO ambiguity



- Electron positron pair is indistinguishable from a photon in a collinear limit
- Which electron should define the muon quantization axis?
- Similar issue: the forward-backward asymmetry and possibly other spin-dependent observables.

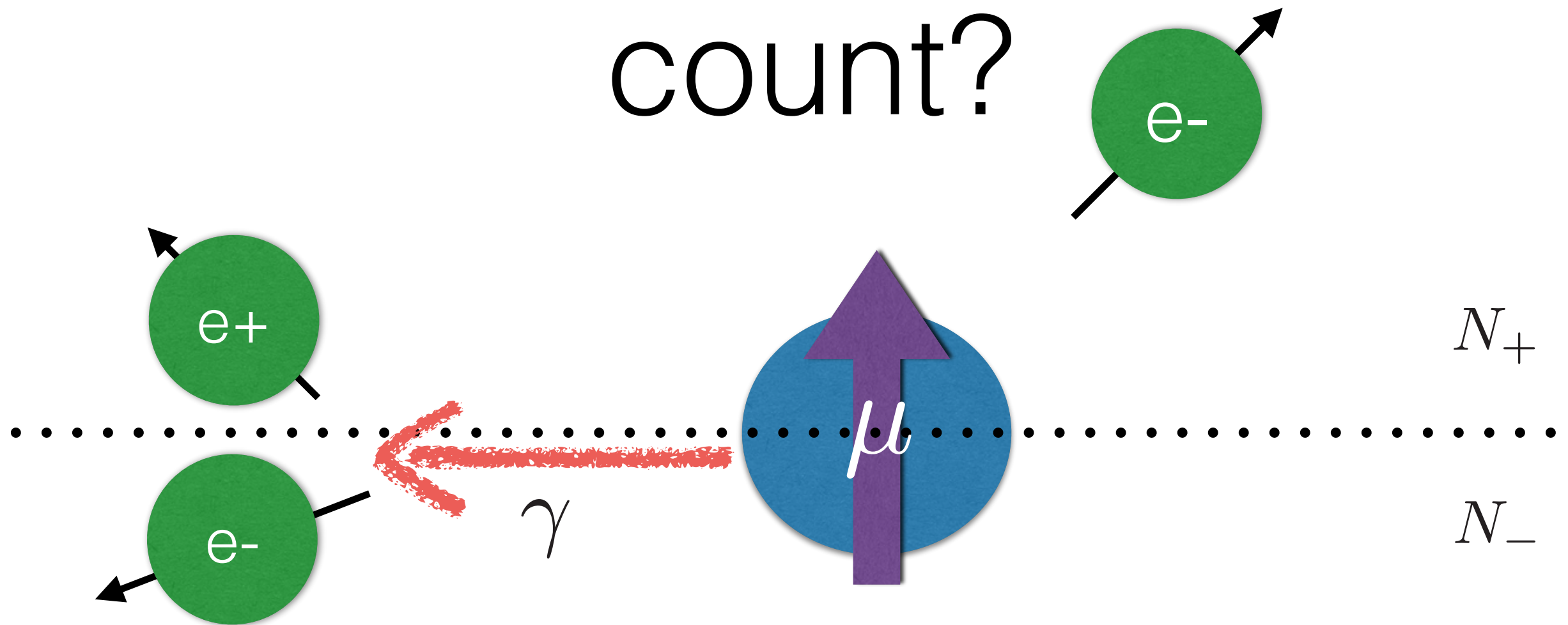
Weinzierl, 2007



Electron positron pair is indistinguishable from a photon in a collinear limit



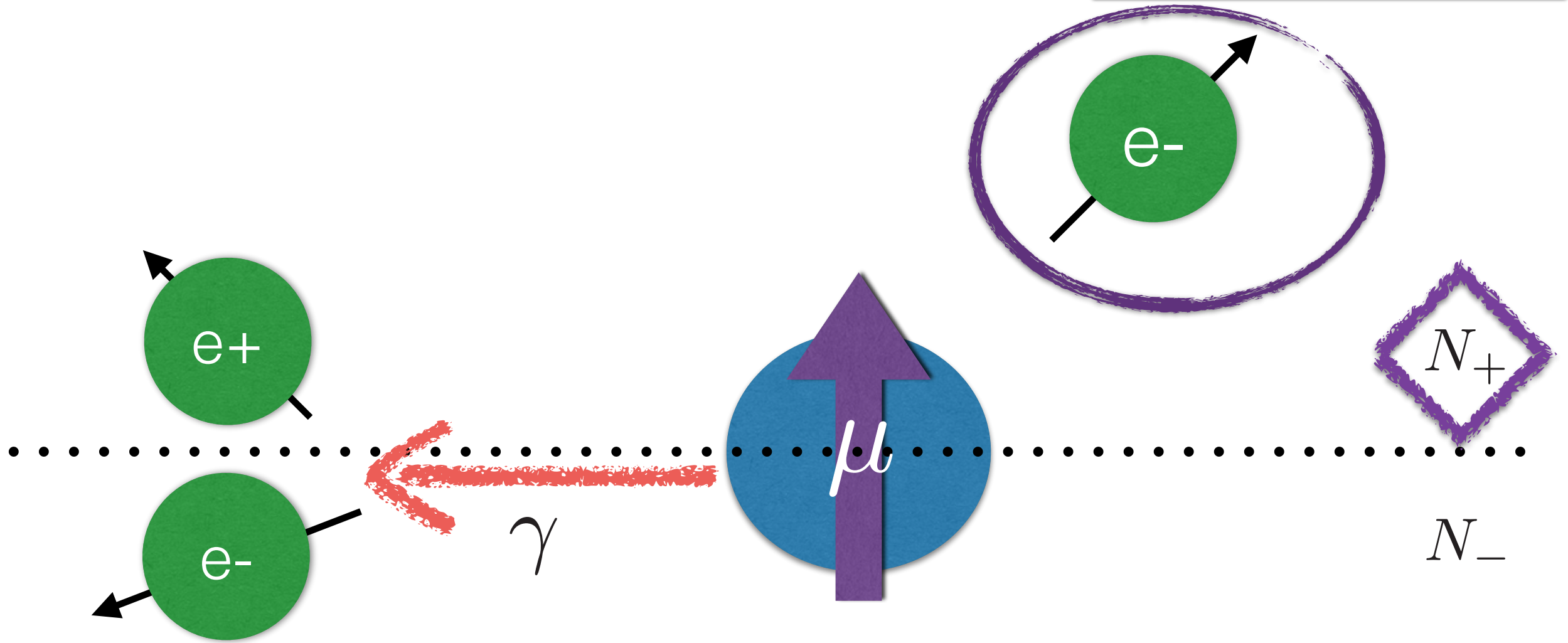
Which electron should we count?



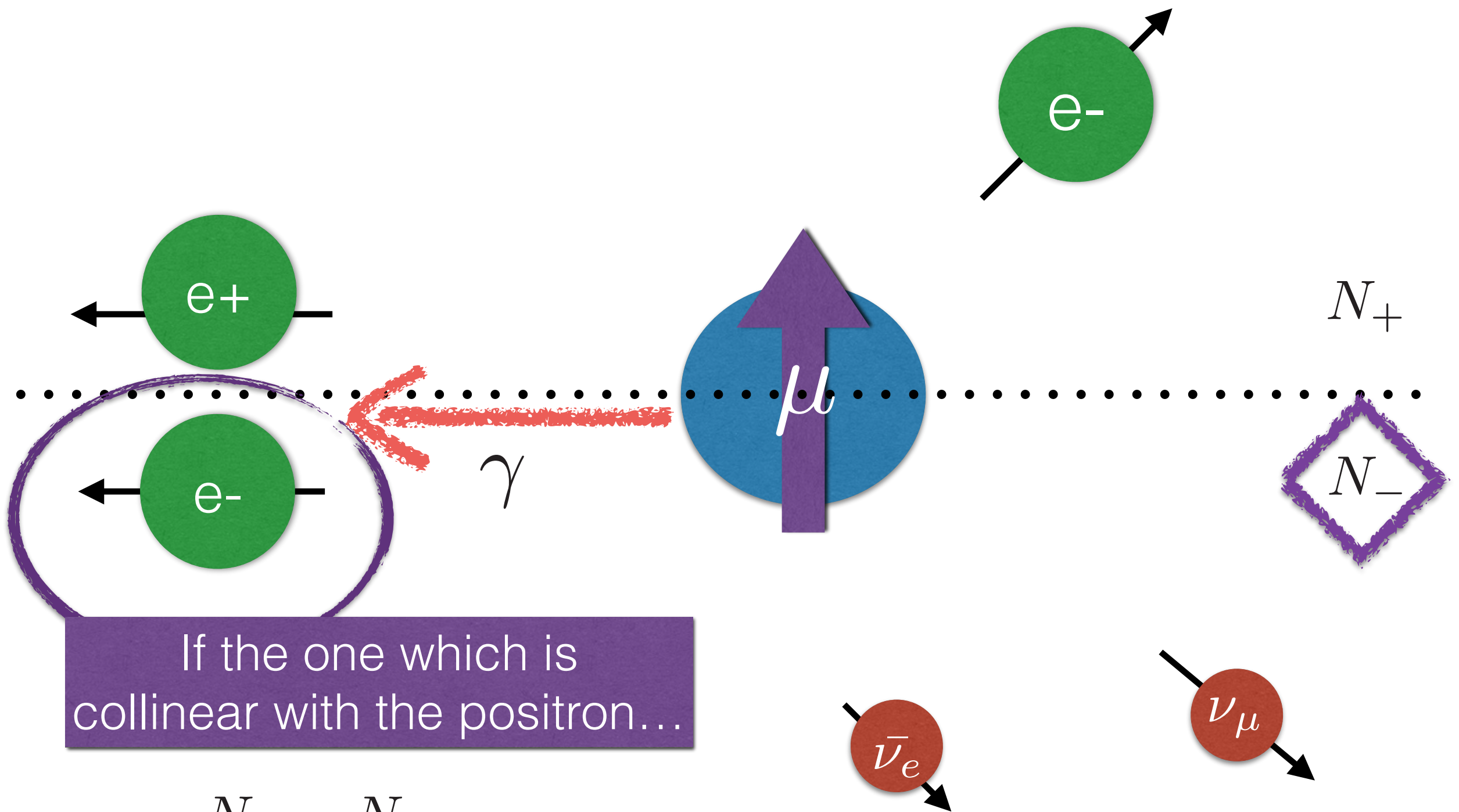
$$A \sim \frac{N_+ - N_-}{N_+ + N_-}$$



If this one, then OK

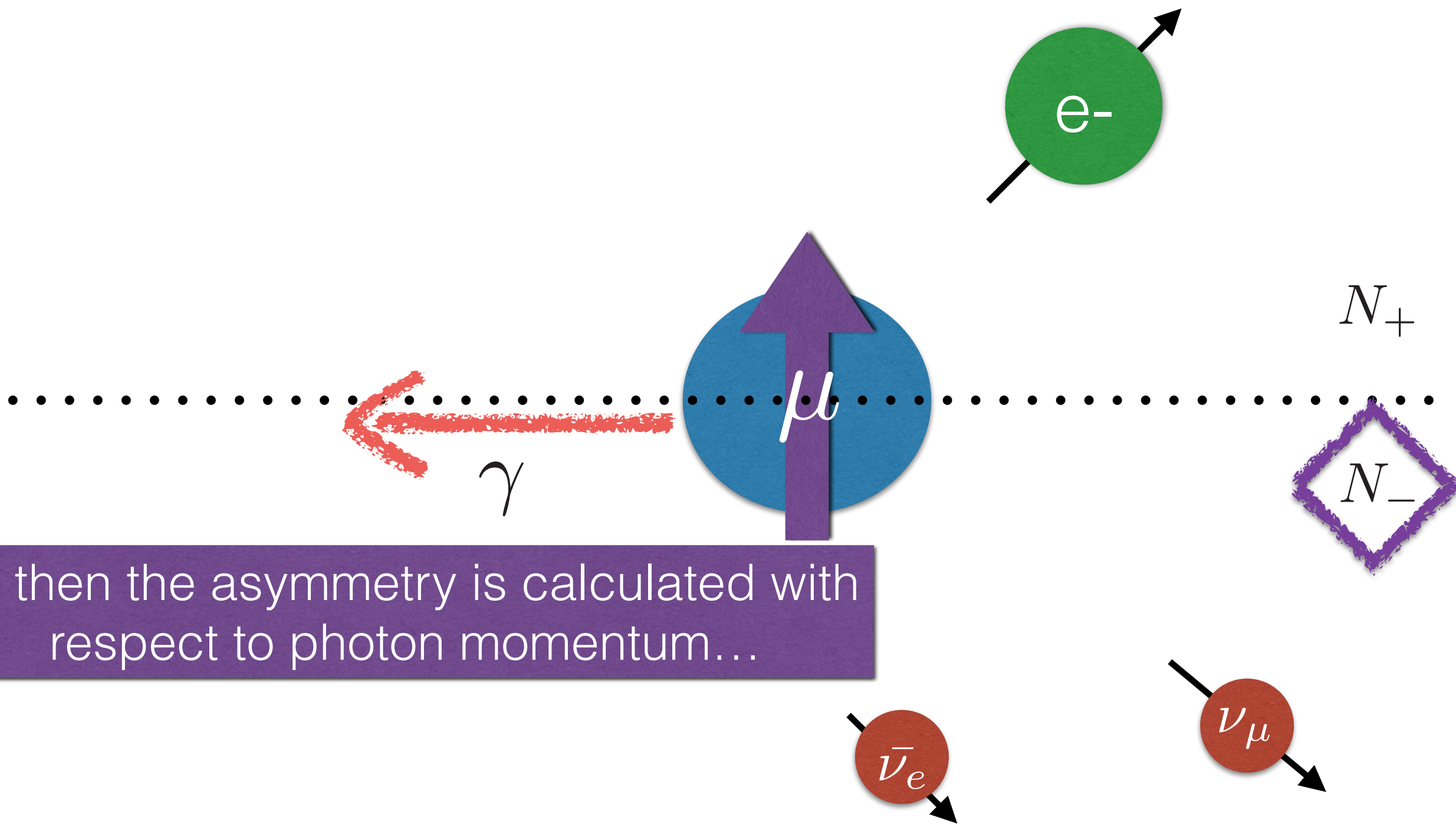


$$A \sim \frac{N_+ - N_-}{N_+ + N_-}$$



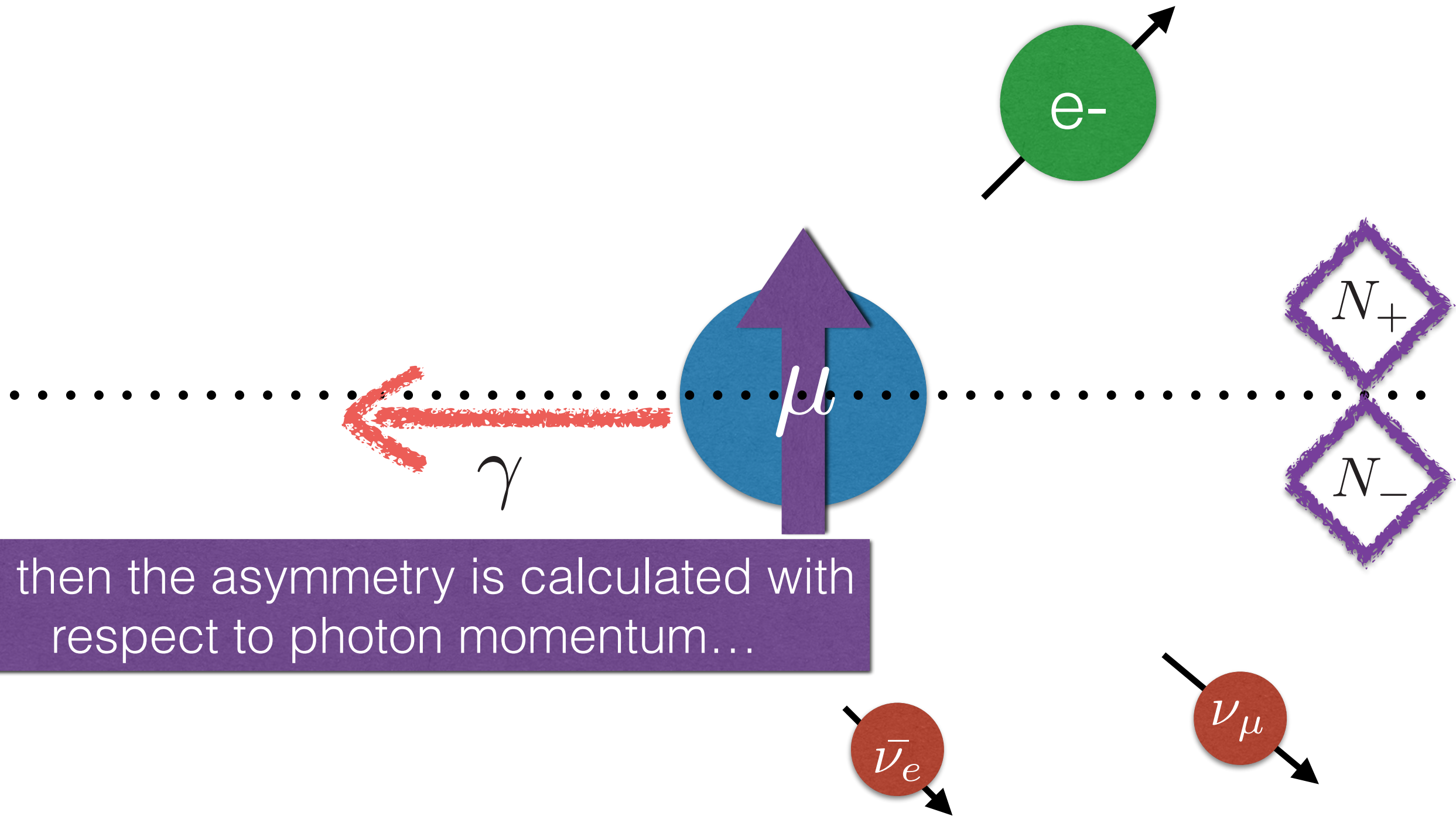
If the one which is collinear with the positron...

$$A \sim \frac{N_+ - N_-}{N_+ + N_-}$$



... then the asymmetry is calculated with respect to photon momentum...

...while in the virtual part there is always one electron and therefore no ambiguity



... then the asymmetry is calculated with respect to photon momentum...

Asymmetry at the NNLO

- Ambiguity makes the asymmetry not an infra-red safe observable (**and we neglected the electron mass!**)
- Large logarithmic corrections to asymmetry at the NNLO
- To solve both problems we invoke the jet concept
 - ▶ Traditional jet algorithms are flavor blind
 - ▶ Durham algorithm allows tracking the jet “flavor”

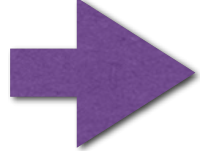
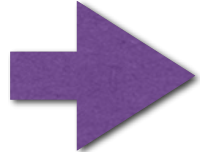
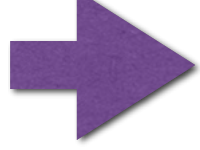
Jet algorithm

Guarantees IR and collinear safety

$$y_{ij}^{(F)} = \frac{2(1 - \cos \theta_{ij})}{m_\mu^2}$$

Banfi, Salam,
Zanderighi, 2006

$$\times \begin{cases} \max(E_i^2, E_j^2), \text{ softer of } i, j \text{ is flavored,} \\ \min(E_i^2, E_j^2), \text{ softer of } i, j \text{ is flavorless.} \end{cases}$$

- Soft photon + Hard electron  electron
- Hard photon + Soft electron  no recombination
- Collinear electron + Positron  photon

Electron jet

- Iteratively recombine if $y_{ij}^{(F)} < y$
- Physically motivated recombination angle $\theta \sim m_e/E_e$
- Typical electron jet size $y \sim \frac{\theta^2 E_e^2}{m_\mu^2} \sim \frac{m_e^2}{m_\mu^2} \sim 2 \times 10^{-5}$
- Expected correction $\sim \alpha^2 \ln 1/y$
- No resummation needed for muon even though

$$\ln 1/y \sim 12$$

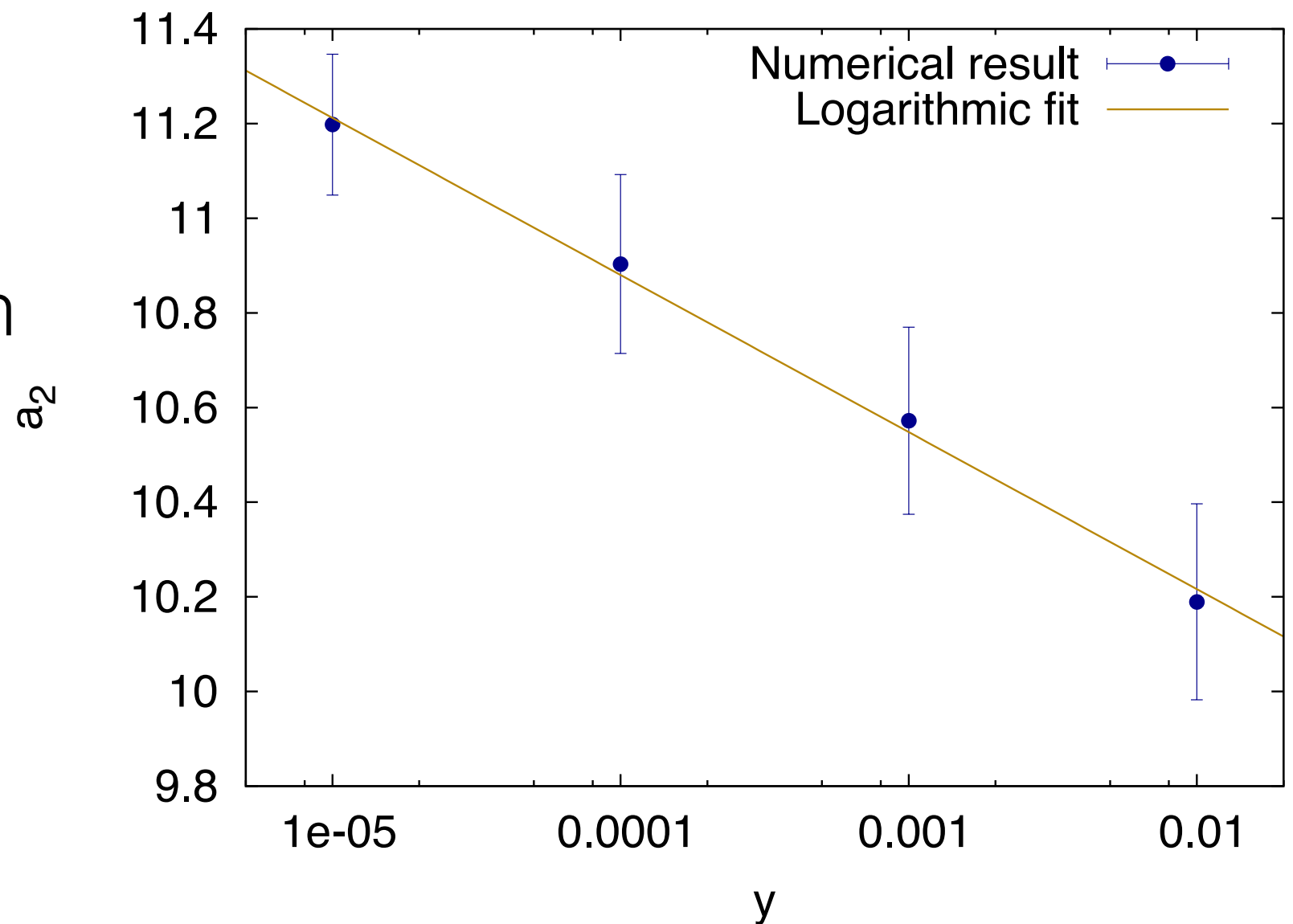
Dependence on the jet resolution

Caola, Czarnecki, Liang,
Melnikov, Szafron, 2014

- Full NNLO calculation
- Neglected electron mass
- Introduced electron jet instead
- Logarithmic part is small for muon

$$m_{\mu} = 105.658\text{MeV}$$

$$a_2 = 9.5(1) - 0.14(1) \ln y$$



Energy dependence

$$A|_{y, E_{min}} = -\frac{1}{3} \left[a_0 + a_1 \frac{\alpha}{\pi} + a_2 \left(\frac{\alpha}{\pi} \right)^2 \right]$$

E_{min}	$a^{(0)}$		$a^{(1)}$		$a^{(2)}$		$\delta_{NLO}, \%$		$\delta_{NNLO}, \%$	
	$y = 10^{-5}$	$y = 10^{-2}$	$y = 10^{-5}$	$y = 10^{-2}$	$y = 10^{-5}$	$y = 10^{-2}$	$y = 10^{-5}$	$y = 10^{-2}$	$y = 10^{-5}$	$y = 10^{-2}$
10 MeV	1.01	1.01	-4.01	-3.25	12.6	11.7	-0.9	-0.8	6.9×10^{-3}	6.4×10^{-3}
20 MeV	1.05	1.05	-5.96	-3.73	21.1	13.8	-1.3	-0.8	1.1×10^{-2}	7.2×10^{-3}
30 MeV	1.05	1.05	-9.24	-4.19	49.3	15.9	-2.1	-0.9	2.6×10^{-2}	8.3×10^{-3}
40 MeV	0.87	0.87	-11.78	-3.79	98.4	14.1	-3.2	-1.0	6.2×10^{-2}	8.9×10^{-3}

Energy dependence

$$A|_{y, E_{min}} = -\frac{1}{3} \left[a_0 + a_1 \frac{\alpha}{\pi} + a_2 \left(\frac{\alpha}{\pi} \right)^2 \right]$$

E_{min}	$a^{(0)}$		$a^{(1)}$		$a^{(2)}$		$\delta_{NLO}, \%$		$\delta_{NNLO}, \%$	
	$y = 10^{-5}$	$y = 10^{-2}$	$y = 10^{-5}$	$y = 10^{-2}$	$y = 10^{-5}$	$y = 10^{-2}$	$y = 10^{-5}$	$y = 10^{-2}$	$y = 10^{-5}$	$y = 10^{-2}$
10 MeV	1.01	1.01	-4.01	-3.25	12.6	11.7	-0.9	-0.8	6.9×10^{-3}	6.4×10^{-3}
20 MeV	1.05	1.05	-5.96	-3.73	21.1	13.8	-1.3	-0.8	1.1×10^{-2}	7.2×10^{-3}
30 MeV	1.05	1.05	-9.24	-4.19	49.3	15.9	-2.1	-0.9	2.6×10^{-2}	8.3×10^{-3}
40 MeV	0.87	0.87	-11.78	-3.79	98.4	14.1	-3.2	-1.0	6.2×10^{-2}	8.9×10^{-3}

- No dependence on the jet resolution in the LO

Energy dependence

$$A|_{y, E_{min}} = -\frac{1}{3} \left[a_0 + a_1 \frac{\alpha}{\pi} + a_2 \left(\frac{\alpha}{\pi} \right)^2 \right]$$

E_{min}	$a^{(0)}$		$a^{(1)}$		$a^{(2)}$		$\delta_{NLO}, \%$		$\delta_{NNLO}, \%$	
	$y = 10^{-5}$	$y = 10^{-2}$	$y = 10^{-5}$	$y = 10^{-2}$	$y = 10^{-5}$	$y = 10^{-2}$	$y = 10^{-5}$	$y = 10^{-2}$	$y = 10^{-5}$	$y = 10^{-2}$
10 MeV	1.01	1.01	-4.01	-3.25	12.6	11.7	-0.9	-0.8	6.9×10^{-3}	6.4×10^{-3}
20 MeV	1.05	1.05	-5.96	-3.73	21.1	13.8	-1.3	-0.8	1.1×10^{-2}	7.2×10^{-3}
30 MeV	1.05	1.05	-9.24	-4.19	49.3	15.9	-2.1	-0.9	2.6×10^{-2}	8.3×10^{-3}
40 MeV	0.87	0.87	-11.78	-3.79	98.4	14.1	-3.2	-1.0	6.2×10^{-2}	8.9×10^{-3}

- No dependence on the jet resolution in the LO
- Weak dependence in the NLO

Energy dependence

$$A|_{y, E_{min}} = -\frac{1}{3} \left[a_0 + a_1 \frac{\alpha}{\pi} + a_2 \left(\frac{\alpha}{\pi} \right)^2 \right]$$

E_{min}	$a^{(0)}$		$a^{(1)}$		$a^{(2)}$		$\delta_{NLO}, \%$		$\delta_{NNLO}, \%$	
	$y = 10^{-5}$	$y = 10^{-2}$	$y = 10^{-5}$	$y = 10^{-2}$	$y = 10^{-5}$	$y = 10^{-2}$	$y = 10^{-5}$	$y = 10^{-2}$	$y = 10^{-5}$	$y = 10^{-2}$
10 MeV	1.01	1.01	-4.01	-3.25	12.6	11.7	-0.9	-0.8	6.9×10^{-3}	6.4×10^{-3}
20 MeV	1.05	1.05	-5.96	-3.73	21.1	13.8	-1.3	-0.8	1.1×10^{-2}	7.2×10^{-3}
30 MeV	1.05	1.05	-9.24	-4.19	49.3	15.9	-2.1	-0.9	2.6×10^{-2}	8.3×10^{-3}
40 MeV	0.87	0.87	-11.78	-3.79	98.4	14.1	-3.2	-1.0	6.2×10^{-2}	8.9×10^{-3}

- No dependence on the jet resolution in the LO
- Weak dependence in the NLO
- Strong dependence in the NNLO

Energy dependence

$$A|_{y, E_{min}} = -\frac{1}{3} \left[a_0 + a_1 \frac{\alpha}{\pi} + a_2 \left(\frac{\alpha}{\pi} \right)^2 \right]$$

E_{min}	$a^{(0)}$		$a^{(1)}$		$a^{(2)}$		$\delta_{NLO}, \%$		$\delta_{NNLO}, \%$	
	$y = 10^{-5}$	$y = 10^{-2}$	$y = 10^{-5}$	$y = 10^{-2}$	$y = 10^{-5}$	$y = 10^{-2}$	$y = 10^{-5}$	$y = 10^{-2}$	$y = 10^{-5}$	$y = 10^{-2}$
10 MeV	1.01	1.01	-4.01	-3.25	12.6	11.7	-0.9	-0.8	6.9×10^{-3}	6.4×10^{-3}
20 MeV	1.05	1.05	-5.96	-3.73	21.1	13.8	-1.3	-0.8	1.1×10^{-2}	7.2×10^{-3}
30 MeV	1.05	1.05	-9.24	-4.19	49.3	15.9	-2.1	-0.9	2.6×10^{-2}	8.3×10^{-3}
40 MeV	0.87	0.87	-11.78	-3.79	98.4	14.1	-3.2	-1.0	6.2×10^{-2}	8.9×10^{-3}

- No dependence on the jet resolution in the LO
- Weak dependence in the NLO
- Strong dependence in the NNLO
- The more inclusive is the observable the weaker is the dependence and the correction smaller

The result

$$\Gamma = \Gamma_0 \left[1 - 1.81 \frac{\alpha}{\pi} + 6.74 \left(\frac{\alpha}{\pi} \right)^2 \right]$$

Total decay width is infrared finite and independent of y .

$$A = A_0 \left[1 - 2.95 \frac{\alpha}{\pi} + 11.2(1) \left(\frac{\alpha}{\pi} \right)^2 \right]$$

Corrections to asymmetry are typically larger than correction to the total decay width

NNLO corrections to asymmetry are more important than the finite electron mass corrections

Part II

Bound muon decay

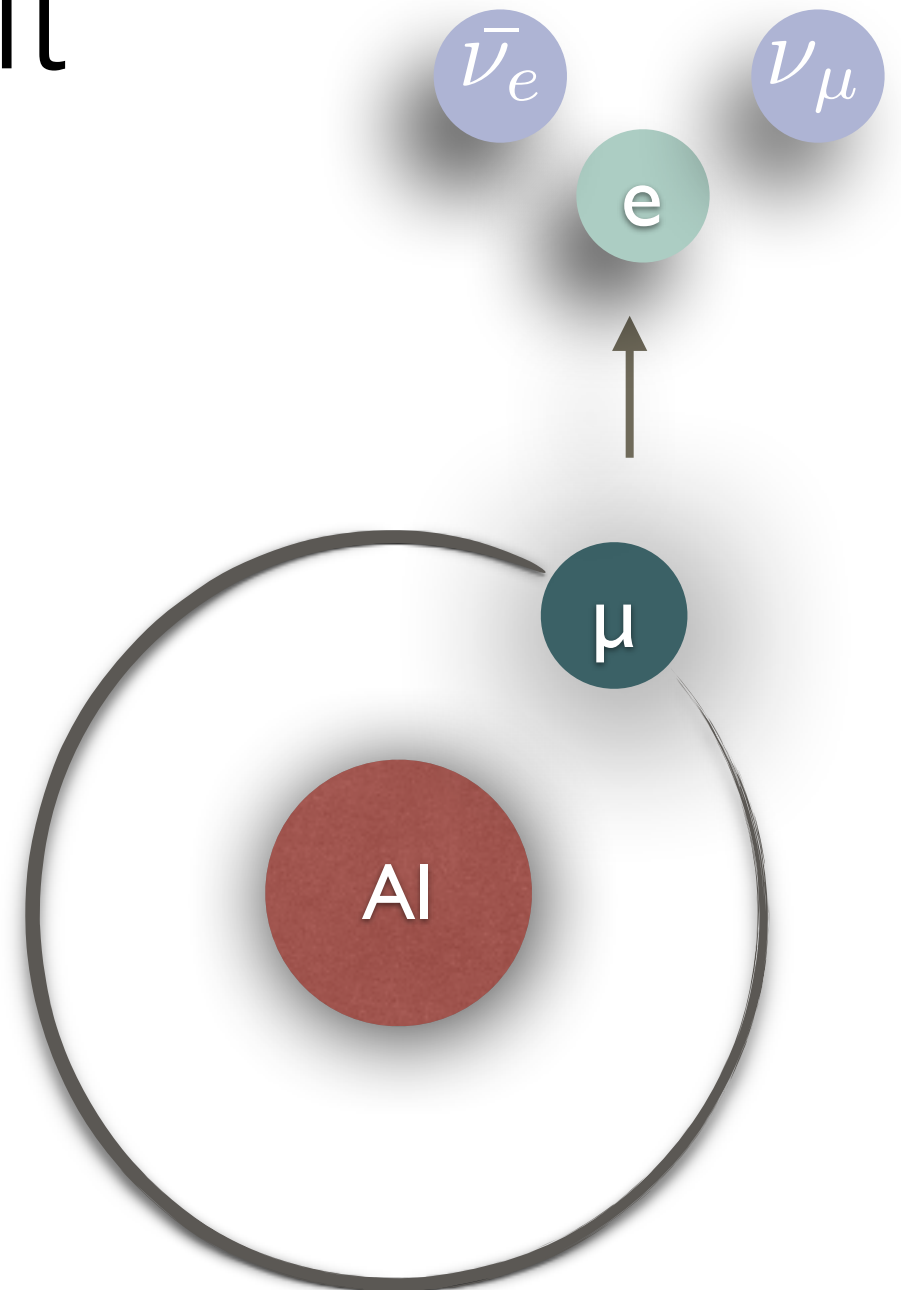
or

What we can learn from
QED about heavy mesons?

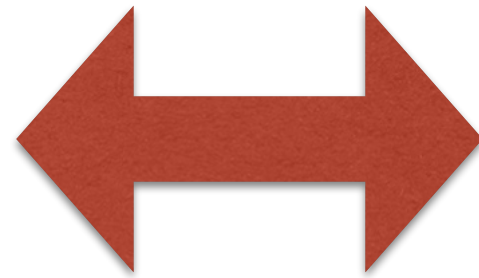
Muon DIO

DIO — Decay In Orbit

- Muon DIO: standard muon decay into an electron and two neutrinos, with the muon and a nucleus forming a bound state
- For DIO momentum can be exchanged between the nucleus and both the muon and the electron

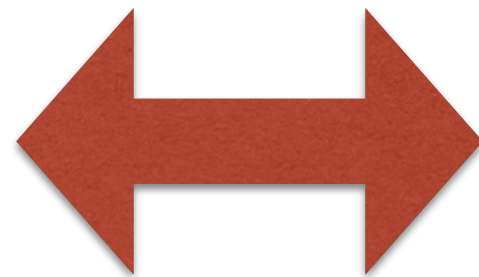


Muon



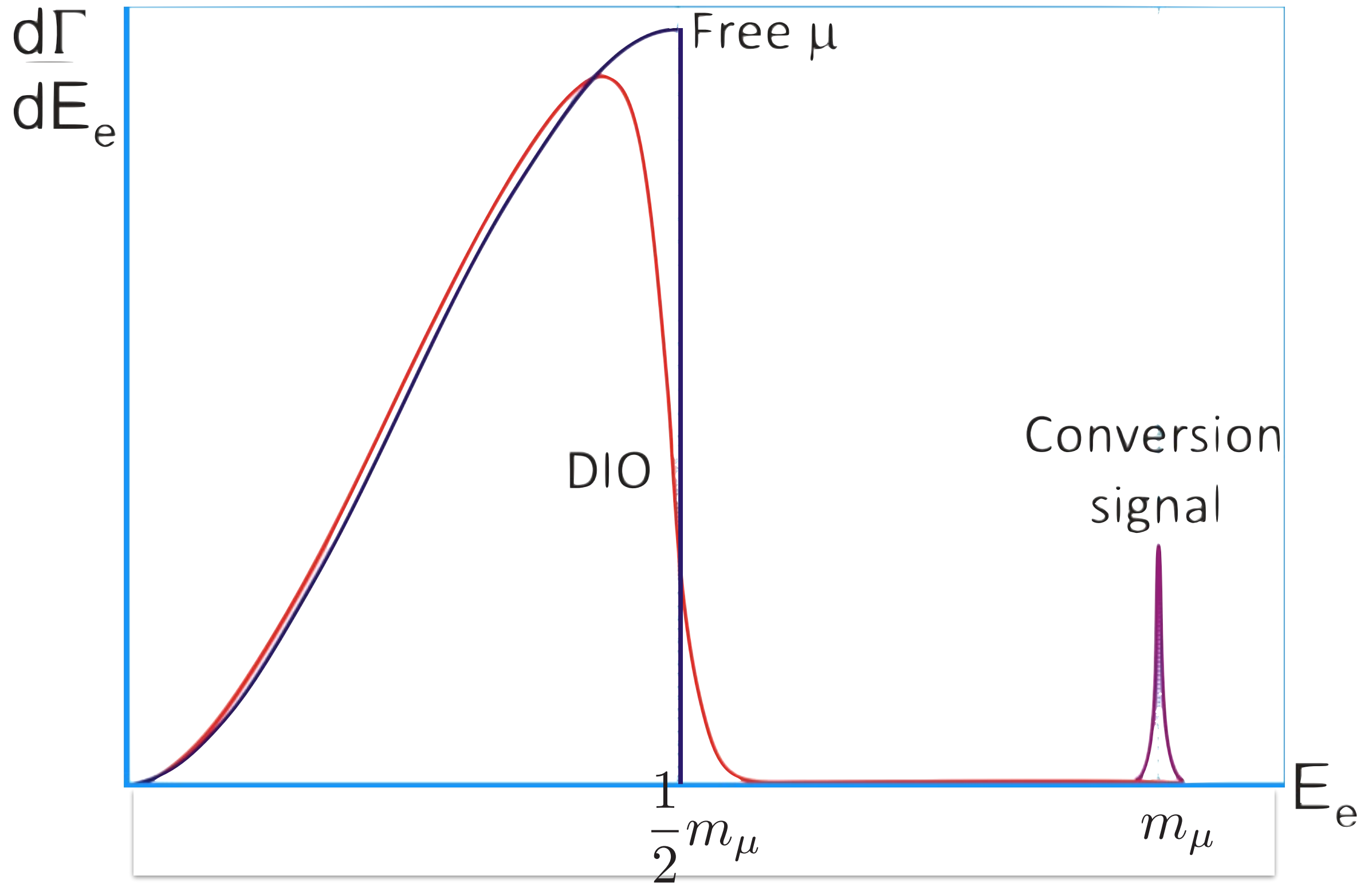
Heavy
quark of
QED

Muonic
atom

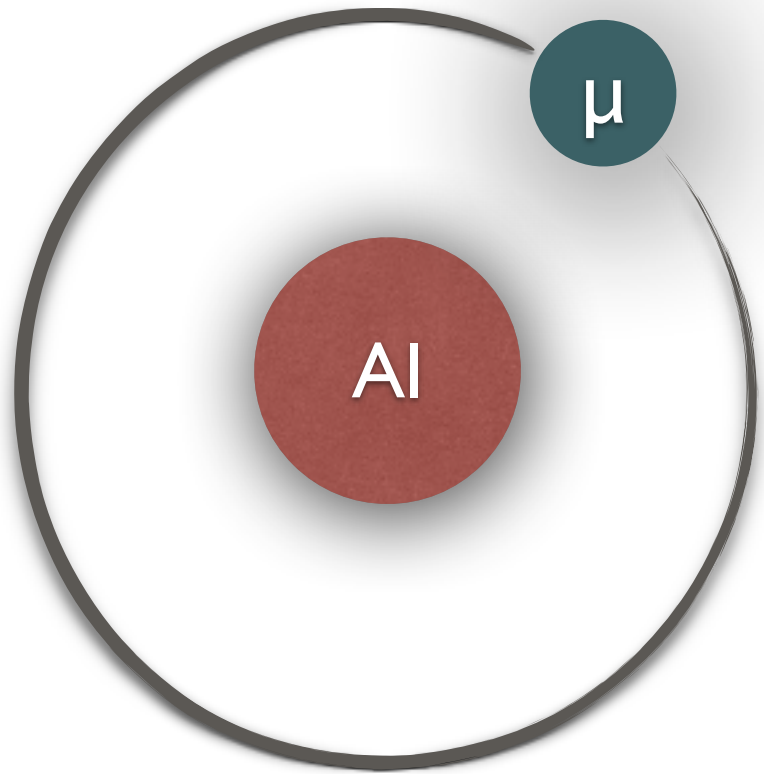


QED
heavy
meson

DIO Spectrum



Characteristic scales of muonic atom



nucleus mass M_{Al}

muon mass m_{μ}

muon momentum $Z\alpha m_{\mu}$

muon binding energy $(Z\alpha)^2 m_{\mu}$

electron cloud $\sim m_e$



$$M_{Al} \gg m_{\mu} \gg m_{\mu} Z\alpha \gg m_{\mu} (Z\alpha)^2$$

Endpoint energy

$$E_{max} = m_{\mu} + E_b + E_{rec}$$

$$E_b \approx -m_{\mu} \frac{(Z\alpha)^2}{2}$$

Binding energy

(+ higher orders)

$$E_{rec} \approx -\frac{m_{\mu}^2}{2m_N}$$

Recoil energy

(kinetic energy of the nucleus)

Both corrections decrease the endpoint energy

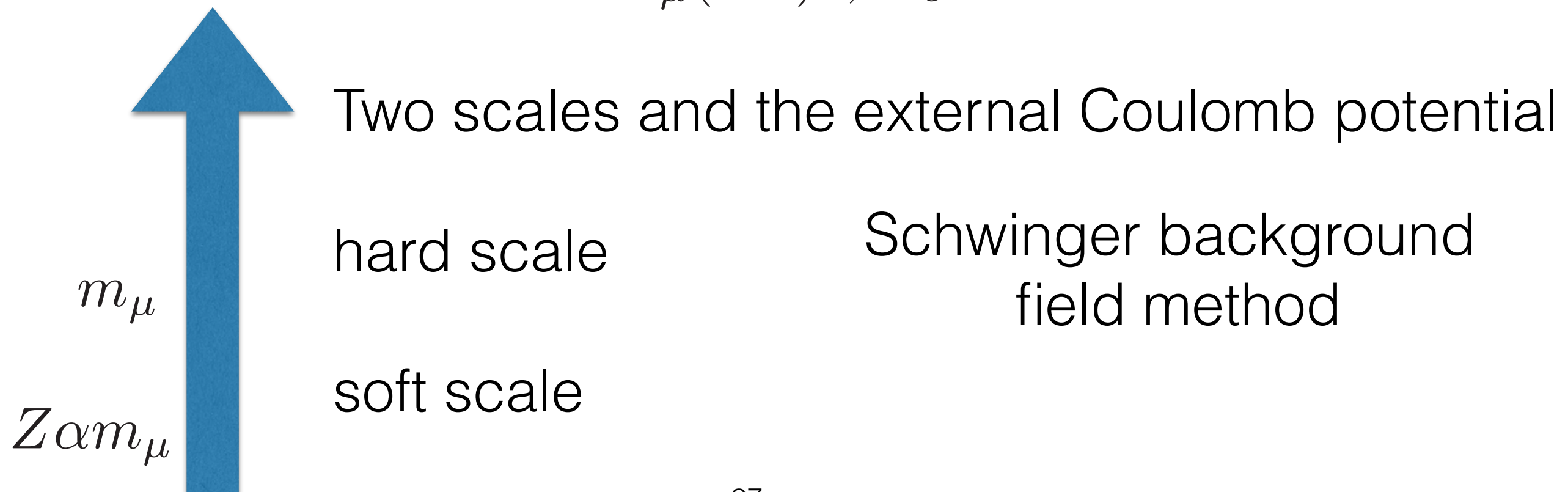
Simplification

- A. Neglect recoil corrections — nucleus is a static source of EM field

$$M_{Al} \rightarrow \infty$$

- B. Neglect higher orders in $Z\alpha$ and m_e

$$m_\mu (Z\alpha)^2, m_e \rightarrow 0$$



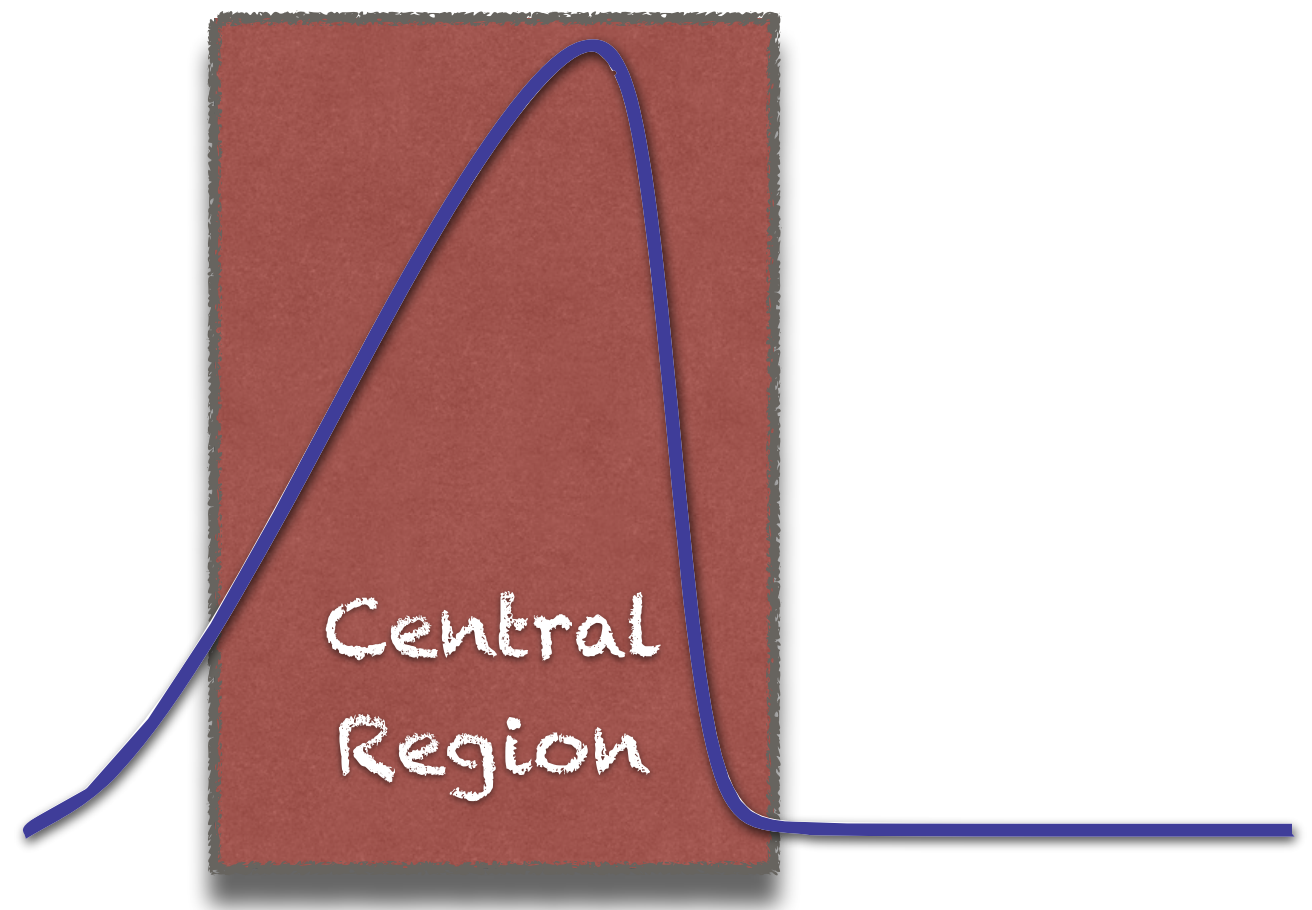
Comparison with mesons containing heavy quarks

- Decay of a heavy particle in the presence of soft background
- No dependence on the nucleus spin in the LO
- Muon momentum $P_\mu = m_\mu v_\mu + k_\mu$ $k \sim m_\mu Z\alpha$

$$m_\mu \longleftrightarrow m_q \quad Z\alpha m_\mu \longleftrightarrow \Lambda_{QCD}$$

How to describe the central region of the spectrum

- Typical momentum transfer between nucleus and muon is of the order of $m_\mu Z\alpha$
- We need resummation
- Dominant effect — muon motion in the initial state



Shape function

In QCD part of the decay spectrum can be described by the shape function

Neubert 1993; Mannel, Neubert 1994; Bigi, Shifman, Uraltsev, Vainshtein, 1994

QED muon shape function

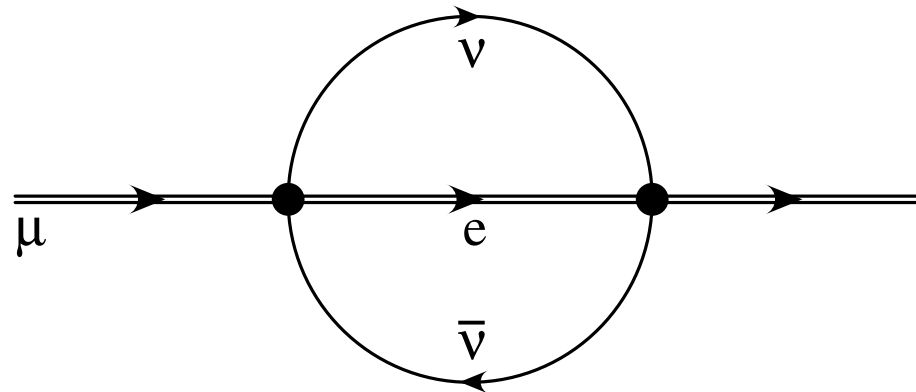
$$S(\lambda) = \int d^3x \psi^*(x) \delta(\lambda - n \cdot \pi) \psi(x)$$

Muon wave-
function

Light-like vector
(electron velocity)

Covariant
derivative

Shape function — basic idea



- Electron propagator in the external field

$$\frac{1}{(p_e + \pi)^2} \approx \frac{1}{p_e^2 + 2p_e \cdot \pi} \rightarrow \delta(p_e^2 + 2p_e \cdot \pi)$$

$$\pi_\mu = i\partial_\mu - eA_\mu$$

- We are interested only in the leading corrections

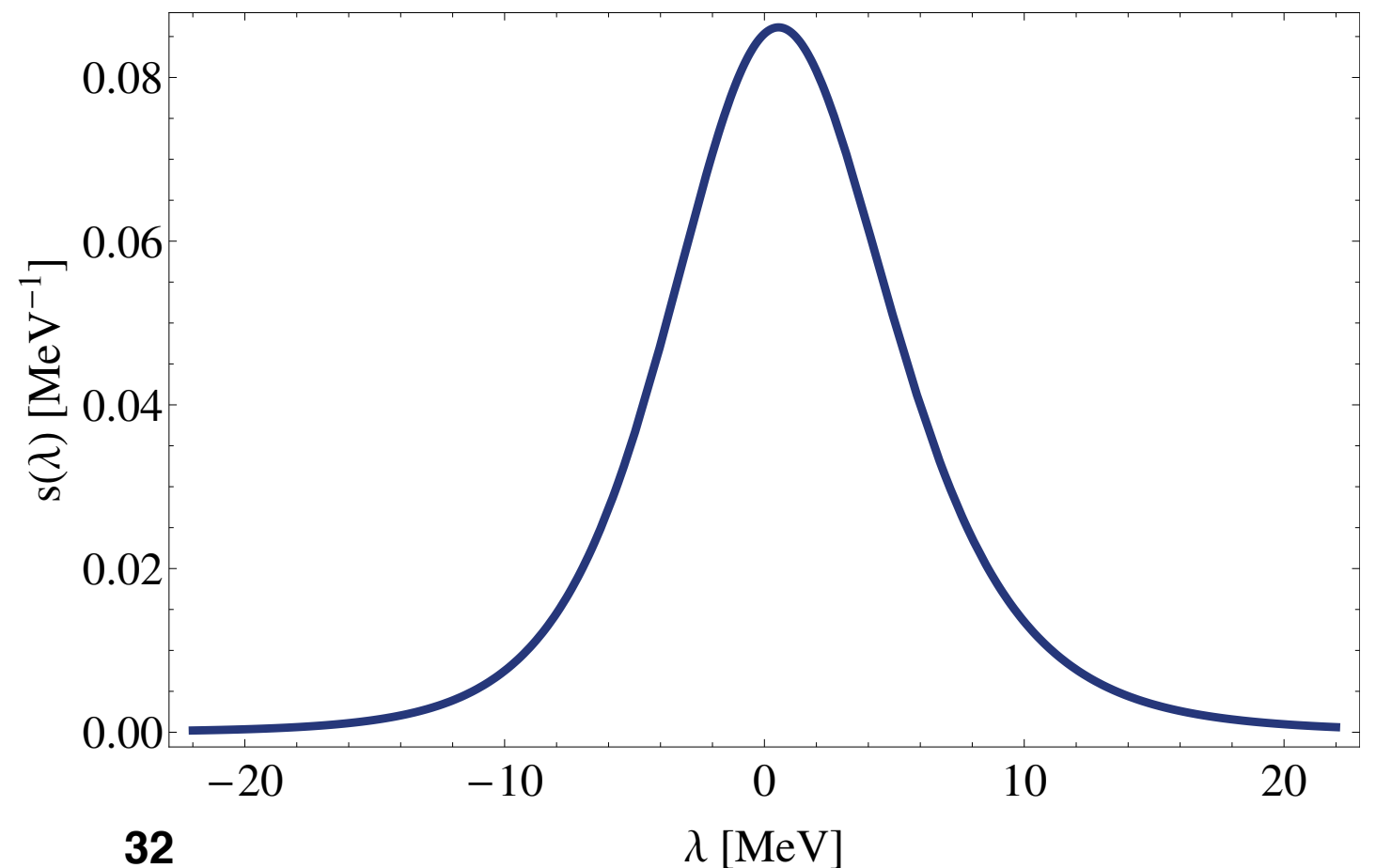
Shape function

For a point-like nucleus the shape function can be calculated analytically

$$S(\lambda) = \frac{8m_{\mu}^5 Z^5 \alpha^5}{3\pi [\lambda^2 + m_{\mu}^2 Z^2 \alpha^2]^3}$$

Szafron, Czarnecki 2015

Shape function describes muon momentum distribution



Power counting

- $\lambda \sim \frac{p_e^2}{2E_e} \sim m_\mu Z\alpha$ (muon momentum in an atom)
- Shape function behaves as $S(\lambda) \sim \frac{1}{Z\alpha}$
- First moment is zero in the leading order

$$\int d\lambda \lambda S(\lambda) = 0$$

Bigi, Uraltsev, Vainshtein, 1992

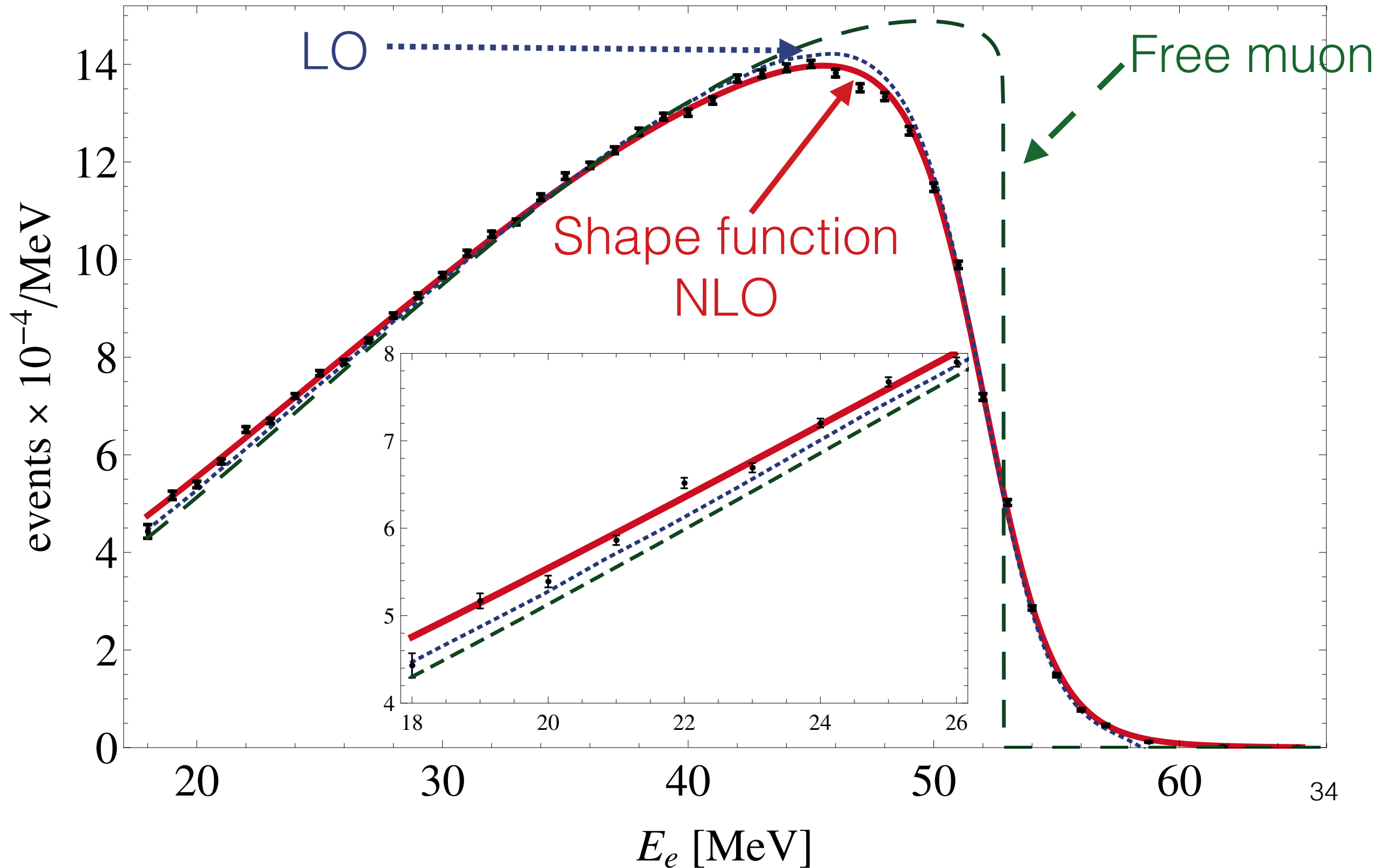
- Second moment $\int d\lambda \lambda^2 S(\lambda) = \frac{1}{3} (m_\mu Z\alpha)^2$

Remember $Z\alpha m_\mu \longleftrightarrow \Lambda_{QCD}$

Results for real atom

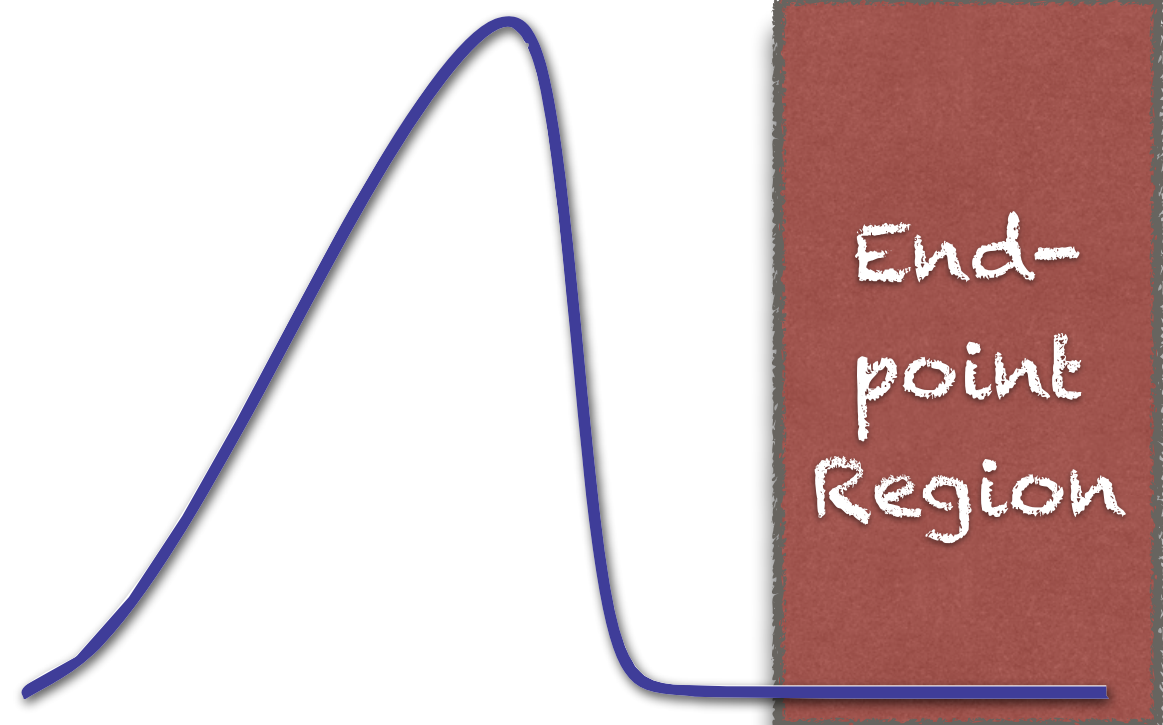
and their relation to the TWIST data

Czarnecki, Dowling,
Garcia i Tormo,
Marciano, Szafron
2014



Endpoint expansion

Near the endpoint the dominant contribution comes from the exchange of hard virtual photons.

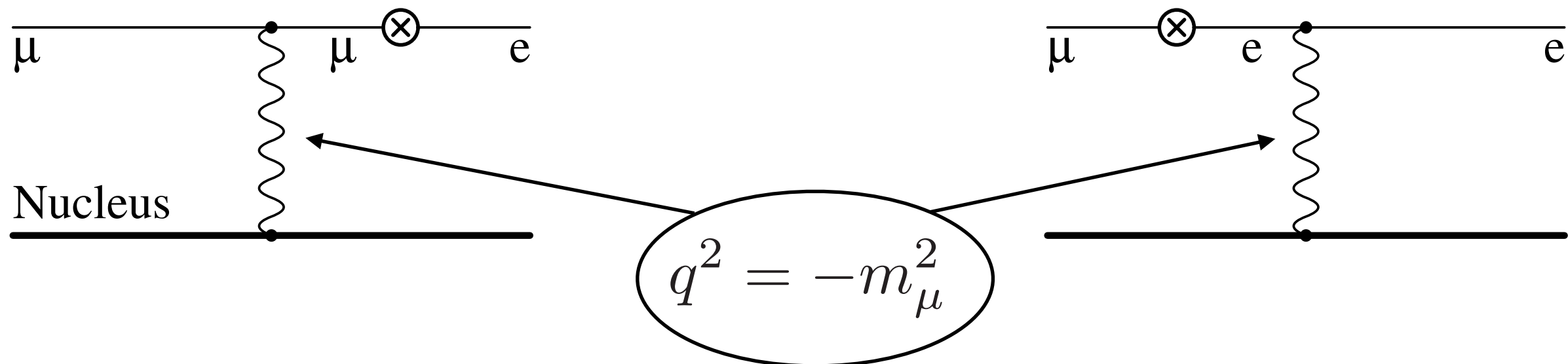


Szafron, Czarnecki 2015

Like a tail of heavy quark spectrum

$$\frac{m_\mu}{\Gamma_{Freee}} \frac{d\Gamma}{dE_e} \approx \frac{1024}{5\pi} (Z\alpha)^5 \left(\frac{\Delta}{m_\mu} \right)^5$$

$$\Delta = E_{max} - E_e$$



Endpoint Radiative corrections

Two large effects:

a) Emission of collinear photons reduces the number of events in the endpoint region

$$\sim \ln \frac{m_\mu}{m_e}$$

b) Large vacuum polarization correction increases the spectrum near the endpoint

$$\frac{1}{m_e} \gg \frac{1}{m_\mu Z \alpha}$$

$$\sim \ln \frac{m_\mu}{m_e} \quad \sim \ln \frac{Z \alpha m_\mu}{m_e}$$

Endpoint region

- Large higher order corrections in $Z\alpha$ ($\sim 20\%$)
- Very sensitive to the nucleus charge distribution ($\sim 50\%$)

Photons with $q^2 = -m_\mu^2$ can probe nucleus interior

Both corrections can be easily incorporated
into the numerical computation

Fragmentation function

$$\frac{d\Gamma_{LL}}{dE_e} = \frac{d\Gamma_{LO}}{dE_e} \otimes D_e$$

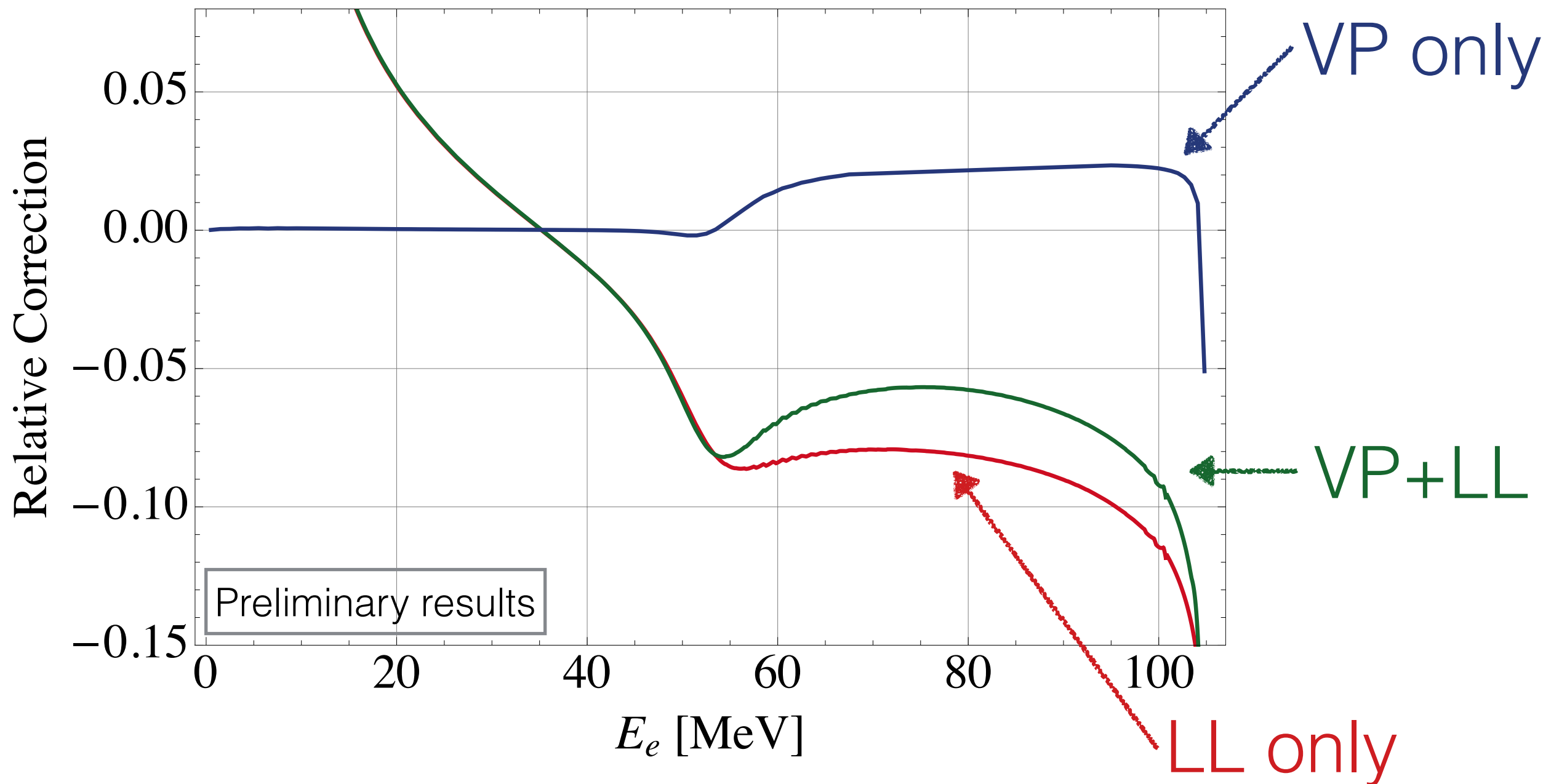
Arbuzov, Czarnecki,
Gaponenko 2002
Arbuzov, Melnikov 2002
Arbuzov, 2003

with the perturbative fragmentation function

$$D_e(x) = \delta(1-x) + \frac{\alpha}{2\pi} \ln\left(\frac{m_\mu^2}{m_e^2}\right) P_{ee}^{(0)}(x) + \dots$$

$P_{ee}^{(0)}(x)$ is the electron splitting function

Leading correction to the DIO spectrum



Summary

- There is a large overlap between methods used to solve different problems
- Large corrections to asymmetry at the NNLO can be expected
- We can improve the DIO spectrum prediction with the help of shape function and fragmentation function and we can better understand the structure functions